ELSEVIER

Journal of Molecular Structure 595 (2001) 67–76

Journal of
MOLECULAR
STRUCTURE

www.elsevier.com/locate/molstruc

Quantum chemical and spectroscopic study of the structure of 2-acetylindan-1,3-dione complexes with metal(II) ions

Venelin Enchev[a,*], Anife Ahmedova[b], Galya Ivanova[a], Iwona Wawer[c], Neyko Stoyanov[d], Mariana Mitewa[b]

[a]*Institute of Organic Chemistry, Bulgarian Academy of Sciences, 1113 Sofia, Bulgaria*
[b]*Department of Chemistry, University of Sofia, 1, J. Bourchier Av., 1126 Sofia, Bulgaria*
[c]*Faculty of Pharmacy, Medical University of Warsaw, Banacha 1, 02097 Warsaw, Poland*
[d]*College of Technology, University of Rousse, 7200 Razgrad, Bulgaria*

Received 1 December 2000; accepted 15 January 2001

Abstract

A series of M(II) (M = Cu, Zn, Cd, Pb) complexes with the physiologically active 2-acetylindan-1,3-dione were synthesized. All complexes were obtained with the metal to ligand ratio 1:2. The presence of two water molecules in the inner coordination sphere of the Zn(II) and Cd(II) complexes was proven. The structure and coordination mode of the newly synthesized Cd(II) and Pb(II) complexes were investigated using NMR (^{13}C CPMAS and ^{13}C NMR in DMF-d_7 solution) method. Semi-empirical (PM3) and ab initio (ECP-31G) calculations of the structure and IR spectra of the free ligand and corresponding metal(II) complexes were performed. It is shown that the structure of the Pb(II) complex differs significantly from the distorted tetrahedral structure of the Cu(II), Zn(II) and Cd(II) complexes. © 2001 Elsevier Science B.V. All rights reserved.

Keywords: 2-Acetylindan-1,3-dione–metal complexes; MO calculations; NMR

1. Introduction

The physiological activity of 2-acetylindan-1,3-dione (2AID) and its derivatives is well documented [1–3]. Its structure has also been studied by X-ray, IR and NMR spectroscopy [4–7]. Recently, some of us have investigated the ground and excited state properties of 2AID using spectroscopic (NMR, UV and fluorescence) and quantum chemical (AM1) methods [8], and have shown evidence of proton transfer occurring in the first excited singlet state. On the other hand, 2AID, being a β-diketone, shows good complexation properties. However, only few data on its complexation properties are available up to now [9–11].

There is no X-ray structure of an 2AID–metal complex in the Cambridge Structural Data Base. The aim of the present paper is to study the composition and structure of a series of metal(II) complexes with 2AID by a combined approach of experimental and quantum-chemical methods.

2. Experimental and calculations

2.1. Synthetic procedures

2-Acetylindan-1,3-dione was obtained by mixing of 0.05 M phthalic anhydride and 0.3 M acetic

---

* Corresponding author. Fax: +359-2-700225.
E-mail address: venelin@orgchm.bas.bg (V. Enchev).

PII: S0022-2860(01)00522-1

anhydride with 0.05 M acetylacetone. The mixture was heated under reflux until the phthalic anhydride was completely dissolved. Then it was cooled to 80°C and 0.15 M triethylamine was added. After 12–14 h, the reaction mixture was poured on 150 g ice with 50 ml concentrated HCl. The resulting precipitate was filtered and washed with water until neutral reaction. The precipitate was dissolved in 500 ml 3% solution of NaOH, and filtered again. The filtrate was acidified with HCl (1:1) resulting in the formation of a precipitate of 2AID. The product was twice recrystalized from ethanol; mp 109–110°C; yield 71%.

The complexes were obtained by mixing methanolic solution of the corresponding metal acetate with ethanolic solution of the ligand. The reaction mixtures were refluxed for about 30 min at 90°C until precipitates were obtained. The latter were washed with ethanol and dried for four weeks above P_4O_{10}. The presence of two water molecules in the Zn(II) and Cd(II) complexes was proved using thermogravimetric analysis. All chemicals were analytical grade reagents.

2.2. IR, EPR and NMR measurements

The IR spectra were recorded on a Perkin–Elmer FTIR-1600 spectrophotometer (KBr tablets). EPR spectra were measured on a Bruker B-ER 420 X-band spectrometer (temperature range 100–300 K). The DTG data were obtained on a Perkin–Elmer TGS-2 instrument.

Cross polarization (CP) magic angle spinning (MAS) solid state ^{13}C NMR spectra were recorded on a Bruker MSL-300 instrument at 75.5 MHz. Powder samples were spun at 8.4 kHz in 4 mm ZrO_2 rotor, a contact time of 4 ms, a repetition time of 6 s and a spectral width of 20 kHz were used for accumulation of 300–600 scans. Chemical shifts were calibrated indirectly through the glycine C=O signal recorded at 176.0 ppm relative to TMS.

The NMR spectra for DMF-d_7 solutions were measured at ambient temperature on a Bruker DRX-250 spectrometer, operating at 250.13 and 62.90 MHz for ^1H and ^{13}C, respectively, using a dual 5 mm probe head. Standard 1D experiments with 30° pulses, 1 s relaxation delay, 16K time domain points, zero-filled to 64K for the protons and 32K for the carbons were performed. The 2D ^1H–^{13}C multiple bond connectivity (HMBC) spectra were recorded with a spectral width of ca. 2000 Hz for ^1H and 15 000 Hz for ^{13}C, relaxation delay 1.5 s, FT size 2K × 256W.

2.3. Quantum-chemical calculations

The PM3 [12,13] calculations were performed for 2AID and its M(II) complexes with Zn, Cd and Pb using the MOPAC 6.0 program [14]. Geometries were optimized without any constrains. The analytic gradient minimization method implemented within an extrapolation procedure called eigenvector following (EF) was used. The mean gradient threshold was 0.01 kcal mol^{-1} $Å^{-1}$. The vibrational analysis of the obtained structures was carried out. The calculated wavenumbers of all normal modes were scaled by a factor of 0.893.

The ab initio structure optimizations for 2AID and its Zn, Cd and Pb complexes were performed at the RHF level. The geometry optimization of the Cu(II) complex was performed at UHF level. Geometric structures were optimized within C_1 symmetry. The calculations described herein were carried out with the Stevens–Basch–Krauss–Jasien effective core potentials (ECP) and their concomitant basis sets for all the atoms (ECP-31G) [15,16]. The ab initio calculations were performed using the GAMESS program package [17]. The IR frequencies for the metal complexes were not calculated because numerical differentiation is a very time-consuming procedure.

3. Results and discussion

The X-ray [4] determined and ab initio calculated structure of 2AID is shown in Fig. 1. There is reasonable agreement between the results obtained by PM3, ab initio (ECP-31G) calculations and crystallographic data (Table 1). According to Antipin et al. [6], the experimental O12···O17 distance in 2AID (at −120°C) is 2.650 Å indicating the presence of the O–H···O intramolecular hydrogen bond. The PM3 and ECP-31G calculations predict this distance to be 2.683 and 2.730 Å, respectively. The ^{13}C NMR data of the solid compound and in DMF-d_7 solution at room temperature are listed in Table 2. A significant downfield shift of the resonance peak of the carbonyl

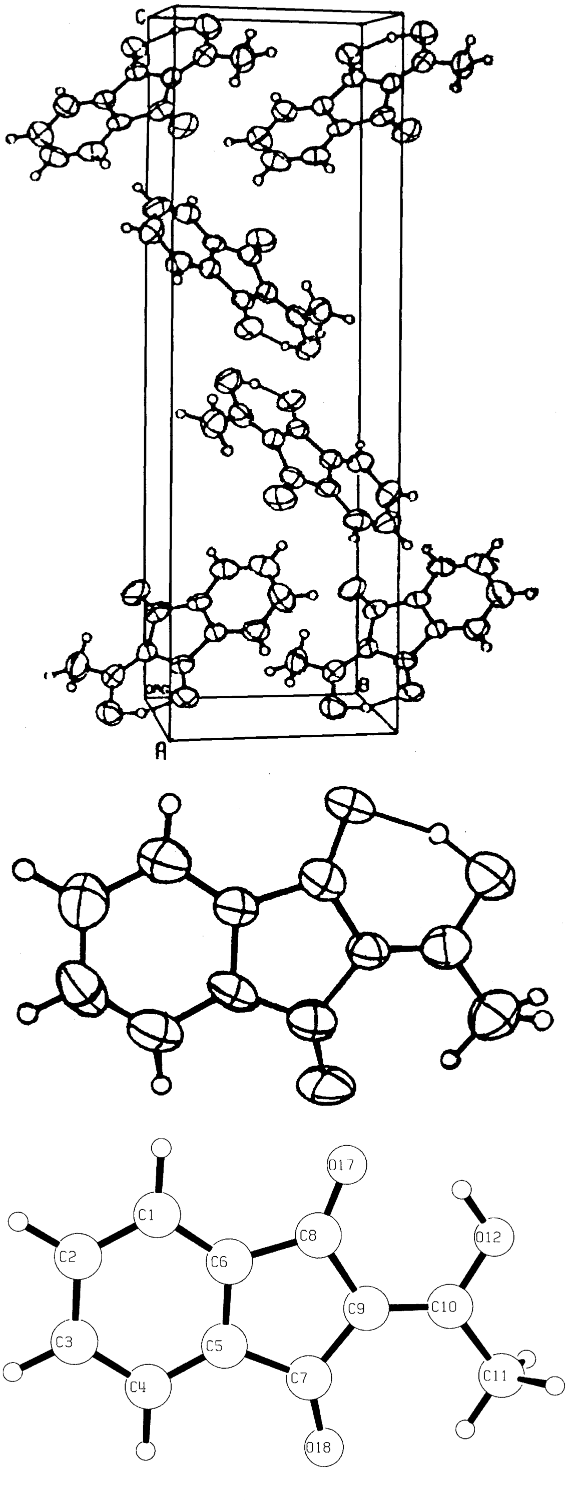

Fig. 1. Stereographic packing diagram, stereographic view and ab initio calculated structure for 2-acetylindan-1,3-dione.

Table 1

Ab initio (ECP-31G) and PM3 calculated structural parameters of 2AID and its compexes with Cu(II), Zn(II), Cd(II) and Pb(II). Bond lengths are in Å, angles in degrees, dipole moments in D and IR frequencies in cm^{-1}. For the numbering of the atoms see Figs. 1 and 3. Available experimental data are also given

Parameter	2AID			$Cu(AID)_2$	$Zn(AID)_2$		$Zn(AID)_2 \cdot 2H_2O$		$Cd(AID)_2$		$Cd(AID)_2 \cdot 2H_2O$		$Pb(AID)_2$	
	Experimental[a]	PM3	ECP	ECP	PM3	ECP	PM3	ECP	PM3	ECP	PM3	ECP	PM3	ECP
Selected distances														
C1–C2	1.386	1.400	1.412	1.416	1.401	1.415	1.401	1.414	1.401	1.415	1.401	1.415	1.400	1.414
C2–C3	1.396	1.388	1.415	1.412	1.387	1.412	1.387	1.413	1.387	1.413	1.387	1.413	1.388	1.413
C3–C4	1.363	1.401	1.413	1.416	1.402	1.416	1.402	1.415	1.402	1.416	1.402	1.415	1.401	1.416
C4–C5	1.394	1.381	1.400	1.396	1.379	1.396	1.379	1.395	1.379	1.397	1.379	1.398	1.380	1.397
C5–C6	1.393	1.411	1.411	1.410	1.410	1.409	1.410	1.409	1.411	1.408	1.411	1.408	1.409	1.409
C6–C1	1.358	1.381	1.401	1.399	1.381	1.398	1.381	1.398	1.380	1.399	1.380	1.399	1.381	1.399
C7–C5	1.475	1.500	1.508	1.513	1.499	1.513	1.500	1.509	1.503	1.512	1.501	1.512	1.499	1.512
C8–C6	1.479	1.486	1.496	1.495	1.494	1.495	1.497	1.491	1.494	1.497	1.492	1.504	1.497	1.498
C9–C7	1.488	1.480	1.490	1.485	1.487	1.487	1.483	1.490	1.476	1.488	1.479	1.483	1.478	1.486
C9–C8	1.448	1.480	1.480	1.441	1.432	1.443	1.430	1.448	1.434	1.447	1.437	1.453	1.455	1.450
C9–C10	1.342	1.367	1.378	1.423	1.412	1.423	1.415	1.415	1.414	1.426	1.408	1.424	1.394	1.415
C10–C11	1.475	1.487	1.507	1.515	1.505	1.515	1.505	1.514	1.501	1.518	1.502	1.521	1.502	1.516
O12–C10	1.352	1.343	1.352	1.291	1.281	1.292	1.275	1.305	1.268	1.291	1.275	1.287	1.285	1.299
O12–H22 (M)	1.140	0.968	0.976	1.950	1.987	1.955	2.025	1.966	2.179	2.172	2.224	2.317	2.083	2.222
O17–H22 (M)	1.560	1.839	1.927	1.978	2.024	1.988	2.062	1.969	2.242	2.213	2.225	2.279	2.754	2.361
O17–C8	1.239	1.224	1.246	1.274	1.266	1.275	1.263	1.274	1.253	1.273	1.252	1.263	1.235	1.267
O18–C7	1.214	1.213	1.235	1.237	1.216	1.236	1.217	1.235	1.218	1.237	1.217	1.240	1.218	1.237
M–O44							2.552	3.835			4.259	2.369		
M–O47							2.552	3.838			4.259	2.378		
Selected bond angles														
C5–C7–O18	126.2	126.3	125.3	124.5	125.7	124.4	125.6	124.5	125.9	124.1	126.0	123.8	125.8	124.3
C6–C8–O17	125.8	128.7	127.0	123.9	120.8	123.3	120.9	123.4	123.4	122.7	123.4	123.0	123.4	123.8
C8–C9–C7	107.5	108.4	108.2	108.1	108.1	108.0	108.4	107.7	108.7	107.9	108.5	108.1	108.4	108.1
C9–C7–O18	128.1	127.8	128.9	129.5	127.9	129.4	128.0	129.4	127.9	129.6	127.7	129.8	127.8	129.5
C9–C8–O17	126.0	124.3	125.8	127.5	130.8	128.1	131.0	127.9	128.6	128.9	128.5	129.1	129.3	128.0
C9–C10–C11	124.9	124.8	126.3	123.0	119.7	123.0	119.3	123.2	119.6	122.6	119.5	122.1	120.2	123.1
C9–C10–O12	121.2	121.6	121.0	120.7	125.7	121.0	125.1	121.1	123.1	121.7	123.5	121.9	124.0	121.4
C10–C9–C7	129.9	129.0	128.8	128.9	123.4	128.6	123.8	128.2	124.8	127.8	124.6	127.7	124.3	128.5
O12–M–O17				89.9	101.7	90.7	97.8	91.6	83.4	81.9	83.4	77.5	75.2	75.3
O12–M–O35				130.1	113.4	119.5	109.5	121.2	123.7	124.4	123.7	121.1	85.0	81.3
O12–M–O23				112.0	115.2	121.7	134.1	113.1	127.8	128.9	127.7	151.8	96.7	91.4
Selected dihedral angles														
C8–O17–M–O23				−116.6	−124.0	−126.9	−150.2	−120.0	−131.7	−132.7	−129.6	−144.6	−87.7	−82.6
C8–O17–M–O35				135.8	121.7	124.9	105.3	126.7	125.2	124.9	127.3	132.3	−39.5	−36.3
C10–O12–M–O23				141.1	122.7	125.1	135.7	130.0	128.2	129.0	126.2	120.9	64.5	70.9
C10–O12–M–O35				−109.2	−120.7	−123.5	−101.4	−122.9	−121.9	−121.7	−123.9	−112.1	138.9	145.8

Table 1 (*continued*)

Parameter	2AID			Cu(AID)$_2$	Zn(AID)$_2$		Zn(AID)$_2$·2H$_2$O		Cd(AID)$_2$		Cd(AID)$_2$·2H$_2$O		Pb(AID)$_2$	
	Experimental[a]	PM3	ECP	ECP	PM3	ECP	PM3	ECP	PM3	ECP	PM3	ECP	PM3	ECP
Dipole moment				4.09 3.54[b]	3.30	4.09 4.69[b]	1.02	7.87	2.64	3.78	4.46	0.84	4.25	3.68
Selected infrared frequencies														
O–H str.		3263												
		3357[c]												
C8=O17 str.		1740					1635				1661		1699	
													1680	
		1653[c]		1616[c]			1617[c]				1619[c]		1630[c]	
													1609[c]	
C7=O18 str.		1795					1773				1775		1774	
													1680	
		1705[c]		1675[c]			1671[c]				1671[c]		1670[c]	
													1694[c]	
C=C str.		1635					1445				1458		1502	
		1592[c]		1576[c]			1579[c]				1581[c]		1566[c]	
g factor														
$g_{\perp}$				2.077[d]										
$g_{\parallel}$				2.276[d]										

[a] X-ray data at room temperature [4].

[b] In dioxan 25°C [10].

[c] In KBr.

[d] At 105 K.

Table 2
^{13}C NMR chemical shifts (ppm) for 2AID and its Cd(II) and Pb(II) complexes in solid state and DMF-d_7 solution. For numbering of the atoms, see Figs. 1 and 3

Carbon	Solid state			Solution		
	2AID	$Cd(2AID)_2{\cdot}2H_2O$	$Pb(2AID)_2$	2AID	$Cd(2AID)_2{\cdot}2H_2O$	$Pb(2AID)_2$
C1	125.0	122.0	119.5	122.4	120.5	122.3
C2	134.4	134.0	132.2	134.7	132.9	133.9
C3	135.0	136.7	132.2	134.7	132.9	133.9
C4	121.8	122.0	122.4	122.4	120.5	122.3
C5	138.2	138.4	137.9	139.6	138.3	138.2
C6	140.2	138.4	134.5	139.6	138.3	138.2
C7	188.6	196.2	192.8	189.1	193.7	193.4
C8	195.9	196.2	195.2	192.4	195.8	194.9
C9	109.3	108.6	113.1	109.0	108.4	109.5
			115.2			
C10	182.9	194.1	188.4	185.1	195.8	189.5
			190.8			
C11	18.3	29.1	32.5	20.4	27.2	24.5
		27.2	28.2			

carbon C8 compared to solution ($\Delta = \delta_{\text{solution}} - \delta_{\text{solid}} = -3.5$ ppm), and an upfield shift of the hydroxyl carbon C10 ($\Delta = 2.1$ ppm) are informative of the existence of a hydrogen-bonded cycle, in agreement with X-ray diffraction results. In the solution spectrum of 2AID, a single resonance appeared for every pair of CH carbons (C2, C3 and C1, C4) and also for the quaternary carbons C5, C6. The formation of the O12–H···O17 hydrogen bond stiffens the molecule and increases its asymmetry. Therefore, in the CPMAS spectrum of solid 2AID, separate resonances for particular carbons are observed (Fig. 2); the signals of C1 and C4 are separated by 3.2 ppm, the signals of C5 and C6 by 2.0 ppm and those of C2 and C3 by 0.6 ppm.

The complexes of 2AID with Cu(II), Zn(II), Cd(II) and Pb(II) were isolated as solid state species (precipitates). The analytical data (Table 3) showed the formation of the complexes with metal to ligand ratio 1:2. Thermogravimetric measurements indicated the presence of two water molecules in the inner coordination sphere of the Zn(II) and Cd(II) complexes. In both cases, mass losses were recorded in the temperature ranges 107–139°C (found 7.83%, calcd 7.75%) and 100–127°C (found 6.40%, calcd 6.89%) for Zn (II) and Cd (II), respectively.

The coordination of the metal ion produces large changes in shielding of the carbons in the vicinity of M(II). The most pronounced effect is observed for C11 (CH_3), downfield shift $\Delta' = \delta_{\text{solid complex}} - \delta_{\text{solid 2AID}}$ amounts to 10.8 or 8.9 ppm for Cd(II) and 14.3 or 9.9 ppm for Pb(II). Smaller differences are observed for C10 [$\Delta' = 11.2$ ppm for Cd(II) and 5.5 or 2.2 ppm for Pb(II)] and C3 [$\Delta' = 0.7$ ppm for Cd(II) and 3.8 or 5.9 ppm for Pb(II)].

Ab initio optimized structures of the Cu(II), Cd(II), Zn(II) and Pb(II) complexes of 2AID are shown in Fig. 3. Selected structural parameters obtained by PM3 and ECP-31G calculations are given in Table 1. There are no considerable differences between the geometry of the free ligand (2AID) and that involved in complexes, except for the fragment where the coordination occurs. The distance C8–C9 (1.480 Å) decreases to 1.441–1.453 Å and C9–C10 (1.378 Å) increases to 1.415–1.426 Å. The C8–O17 bond becomes longer, in contrast to the C10–O12 one, as a result of the coordination. The C10–O12 (1.352 Å) bond lengths decrease to 1.287–1.305 Å and the C8–O17 (1.246 Å) increase to 1.263–1.275 Å. The last two changes explain the differences in the IR spectra of the free ligand and the corresponding complexes. In this way, the lengths of the double and single bonds in the so formed chelate ring are averaged.

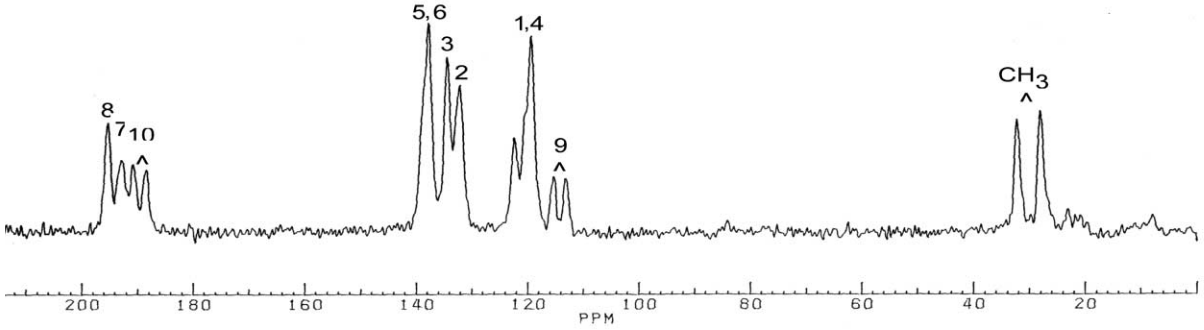

Pb(2AID)$_2$ complex

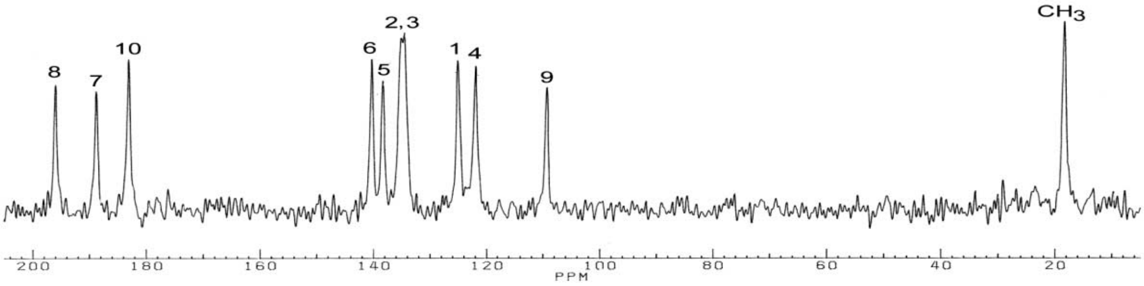

2-acetylindan-1,3-dione

Fig. 2. ^{13}C CPMAS NMR spectrum of solid 2-acetylindan-1,3-dione and Pb(2AID)$_2$ complexes.

The distances O17–M and O12–M depend on the metal ion radii. The oxygen atoms coordinated to M(II) are not coplanar with it (see the dihedral angles in Table 1) and the complexes have a distorted (flattened) tetrahedral structure.

The Cu(II) complex is paramagnetic and EPR active. The EPR spectrum recorded at different temperatures (100–300 K, a powder sample) is typical for Cu(II) (d_9) complexes with lower symmetry, showing partially resolved two-component anisotropy. No hyperfine structure (hfs) was observed due to $^{63.65}$Cu ($I = 3/2$) (Table 1). These data prove the distorted tetrahedral structure for the Cu(II) complex. The latter is typical for Cu(II) complexes due to the Jahn–Teller effect.

According to the quantum-chemical calculations,

Table 3
Elemental analyses data of the complexes

Complex	Molecular formula	C (%)		H (%)	
		Calculated	Found	Calculated	Found
Cu(AID)$_2$	$C_{22}H_{14}O_6Cu$ (437.90)	60.4	60.3	3.2	3.0
Zn(AID)$_2$·2H$_2$O	$C_{22}H_{18}O_8Zn$ (475.77)	55.4	55.7	3.8	3.3
Cd(AID)$_2$·2H$_2$O	$C_{22}H_{18}O_8Cd$ (522.79)	50.5	50.0	3.5	3.0
Pb(AID)$_2$	$C_{22}H_{14}O_6Pb$ (581.55)	45.4	45.6	2.4	2.1

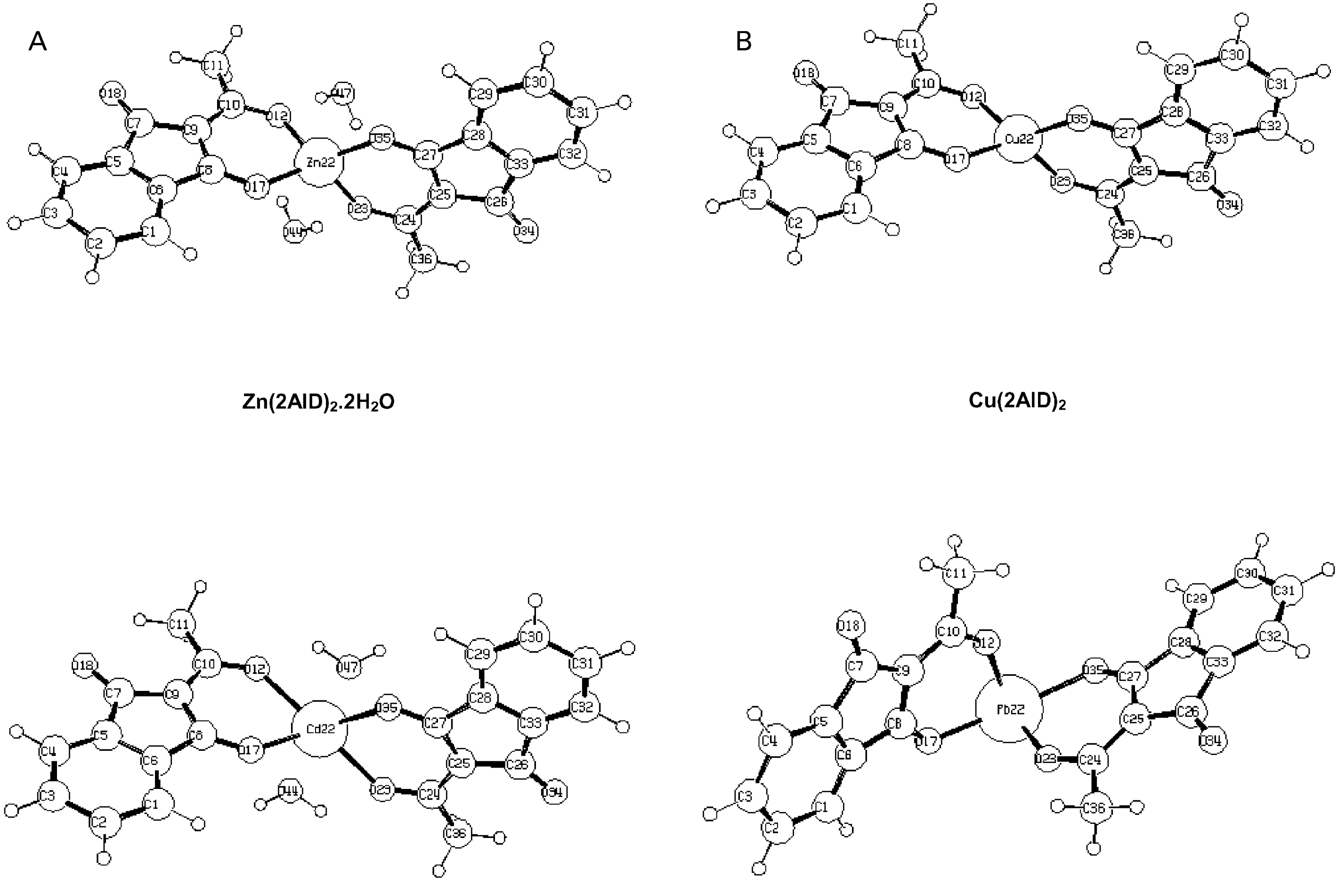

Zn(2AID)$_2$.2H$_2$O

Cu(2AID)$_2$

Cd(2AID)$_2$.2H$_2$O

Pb(2AID)$_2$

Fig. 3. Ab initio (ECP-31G) calculated structures of the Zn(2AID)$_2$·2H$_2$O, Cd(2AID)$_2$·2H$_2$O (Fig. 3a), Cu(2AID)$_2$ and Pb(2AID)$_2$ (Fig. 3b) complexes.

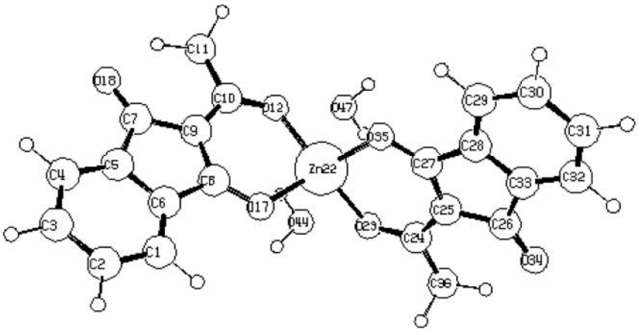

$Zn(2AID)_2.2H_2O$

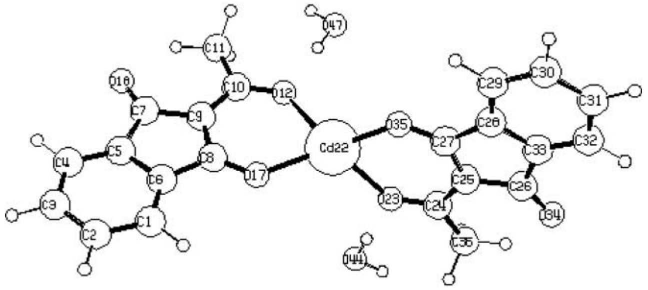

$Cd(2AID)_2.2H_2O$

Fig. 4. PM3 calculated structures of the $Zn(2AID)_2{\cdot}2H_2O$ and $Cd(2AID)_2{\cdot}2H_2O$ complexes.

the two ligands in the $Pb(2AID)_2$ complex lie in approximately perpendicular planes (see the dihedral angle C8–O17–M–O23, Table 1). This result could explain the appearance of two signals for C9, C10 and C11 (Table 2) separated by 2.1, 2.4 and 4.3 ppm, respectively, in the ^{13}C CPMAS NMR spectrum. Additional signals in the spectrum of solid $Cd(2AID)_2{\cdot}2H_2O$, best seen for the C11 of methyl group, indicate that in this case also, the two ligands are not equivalent, most likely due to interaction with the water molecule.

Ab initio and PM3 calculations were also performed for $Zn(2AID)_2$ and $Cd(2AID)_2$ in the presence of two water molecules in the inner coordination sphere (according to DTA data; Table 3). The results are shown in Figs. 3 and 4, respectively. IR evidence for the presence of water molecules in the Zn(II) and Cd(II) complexes is also available — a very broad band at $\sim 3500\ \mathrm{cm}^{-1}$ corresponding to a stretching vibration and a middle intensive band at $\sim 1550\ \mathrm{cm}^{-1}$ corresponding to a bending vibration in water are observed.

The PM3 and ECP calculated geometries of the Zn(II) and Cd(II) complexes in presence of two water molecules in the inner coordination sphere leads to changes in the metal–oxygen bond lengths, in comparison with $\mathrm{Zn(2AID)_2}$ and $\mathrm{Cd(2AID)_2}$. PM3 results for $\mathrm{Zn(2AID)_2{\cdot}2H_2O}$ show that both the bond lengths M–O12 and M–O17 increase by 0.038 Å. However, in the case of the $\mathrm{Cd(2AID)_2{\cdot}2H_2O}$, M–O12 becomes longer (by 0.045 Å) and the M–O17 bond becomes shorter by 0.017 Å. A similar result is obtained for the ECP optimized $\mathrm{Zn(2AID)_2{\cdot}2H_2O}$: a small increase in the M–O12 bond length (0.011 Å) and a decrease in the M–O17 bond length (0.019 Å). In the case of the $\mathrm{Cd(2AID)_2{\cdot}2H_2O}$, ECP calculations show a strong increase in both M–O12 and M–O17 bond lengths by 0.135 and 0.066 Å, respectively. The latter become longer than the corresponding ones in $\mathrm{Pb(2AID)_2}$, even though the metal ion radius of the Pb(II) is greater.

References

[1] C.H. Hassal, Experentia 6 (1950) 462.

[2] L.W. Hazleton, W.H. Dolben, USA Patent 2 884 357, 1959.

[3] J.T. Correll, L.L. Coleman, St. Long, R.F. Willy, Proc. Soc. Exp. Biol. Med. 80 (1952) 139.

[4] J.D. Korp, I. Bernal, T.L. Lemke, Acta Crystallogr. B 36 (1980) 428.

[5] M.V. Petrova, E.E. Liepins, J.J. Paulins, I.Ya. Gudele, E.Yu. Gudriniece, Izv. Acad. Nauk Latv. SSR, Ser. Khim. (1987) 601.

[6] M.Yu. Antipin, M.V. Petrova, Ya.Ya. Paulins, Yu.T. Struchkov, E.Yu. Gudriniece, Izv. Acad. Nauk Latv. SSR, Ser. Khim. (1989) 102.

[7] E. Liepins, M.V. Petrova, E. Gudriniece, J. Paulins, S.L. Kuznetsov, Magn. Res. Chem. 27 (1989) 907.

[8] V. Enchev, S. Bakalova, G. Ivanova, N. Stoyanov, Chem. Phys. Lett. 314 (1999) 234.

[9] D. Zacharova-Kalavska, A. Perjessy, I. Zelensky, Coll. Czech. Chem. Commun. 35 (1970) 225.

[10] T.L. Usova, O.A. Osipov, L.S. Minkina, V.G. Zaletov, Koord. Khim. 9 (1983) 879.

[11] K.P. Butin, R.D. Rakhimov, I.G. Il'ina, Izv. Acad. Nauk, Ser. Khim. (1999) 71.

[12] J.J.P. Stewart, J. Comput. Chem. 10 (1989) 209.

[13] J.J.P. Stewart, J. Comput. Chem. 12 (1991) 320.

[14] J.J.P. Stewart, MOPAC 6.0, QCPE No. 455, Bloomington, IN, 1990.

[15] W.J. Stevens, H. Basch, M. Krauss, J. Chem. Phys. 81 (1984) 6026.

[16] W.J. Stevens, H. Basch, M. Krauss, P. Jasien, Can. J. Chem. 70 (1992) 612.

[17] M.W. Schmidt, K.K. Baldridge, J.A. Boatz, S.T. Elbert, M.S. Gordon, J.H. Jensen, S. Koseki, N. Matsunaga, K.A. Nguen, S. Su, T.L. Windus, M. Dupuis, J.A. Montgomery Jr., J. Comput. Chem. 14 (1993) 1347.